Journal of Manufacturing Systems 33 (2014) 76–83

Contents lists available at ScienceDirect

Journal of Manufacturing Systems

journal homepage: www.elsevier.com/locate/jmansys

Model testing of fixture–workpiece interface compliance in dynamic conditions

Branko Tadic[a], Djordje Vukelic[b,*], Dragomir Miljanic[c], Bojan Bogdanovic[a], Ivan Macuzic[a], Igor Budak[b], Petar Todorovic[a]

[a] University of Kragujevac, Faculty of Engineering, Department for Production Engineering, 34000 Kragujevac, Serbia
[b] University of Novi Sad, Faculty of Technical Sciences, Department for Production Engineering, 21000 Novi Sad, Serbia
[c] Metalik DOO, Trebjeska 6, 81400 Niksic, Montenegro

ARTICLE INFO

Article history:
Received 1 November 2012
Received in revised form 21 January 2013
Accepted 20 May 2013
Available online 15 June 2013

Keywords:
Fixture
Machining
Clamping
Locating
Compliance

ABSTRACT

This paper is focused on the problem of compliance of interface between clamping/locating fixture elements and workpiece, under dynamic loads during machining. In contrast to previous investigations, the authors have developed a special device dedicated to testing of physical models which represent clamping/locating elements and workpiece. This device allows optimization of a large number of input parameters which are critical to interface compliance. It was used in experimental investigations to establish the impact that the radius of the spherical tip of a clamping/locating element has on the interface compliance and load capacity. The results of experimental investigation show that, under certain conditions, the clamping/locating elements with larger-radius spherical tips provide significantly lower interface compliance. Future investigations should be aimed at finding optimum macro- and micro-geometries of contact interface, as well as the selection of materials for clamping/locating elements.

1. Introduction

The main objective of machining fixture is to establish and secure the desired position and orientation of the workpiece during machining on machine tool. Fixtures have a direct impact upon product quality, productivity and cost. The costs associated with fixture planing, design and manufacture can account for 10–20% of the total cost of a manufacturing system [1]. On the other hand, approximately 40% of rejected parts are due to dimensioning errors that are attributed to poor fixturing design [2].

Many researchers have focused on the investigation of the influence of fixture–workpiece system on the aggregate accuracy of machining. As regards the fixture layout optimization, the research has been mostly focused on: kinematic analysis, force analysis, contact analysis, finite-element analysis (FEA), etc. Numerous methodologies have been proposed to allow fixture layout optimization.

Meyer and Liou [3] presented a methodology to generate fixture layout under dynamic machining forces. Linear programming was used to determine optimal positions of locating elements and clamping forces. Nee et al. [4] reported a sensor-assisted fixture that was capable of delivering varying clamping loads, calculated from a quasi-static model, to minimize workpiece distortion. Li and Melkote [5] presented an optimal synthesis approach for the fixture layout and clamping force that considers workpiece dynamics during machining and determines the optimal clamping force for a multiple clamp fixture subjected to a quasi-static machining force. Hurtado and Melkote [6] formulated a multi-objective optimization model that defines minimum clamping loads to achieve workpiece shape conformability and fixture stiffness goals for a workpiece subjected to quasi-static machining forces. Kulankara et al. [7] presented an iterative algorithm that minimized the workpiece elastic deformation for the entire cutting process by alternatively varying the fixture layout and clamping force. Vallapuzha et al. [8] investigated the use of spatial coordinates to represent locations of fixture elements in their fixture layout optimization model solved by genetic algorithms (GA). Xiong et al. [9] formulated the clamping optimization problem as a constrained nonlinear programming problem based on the concept of passive force closure. Kaya and Ozturk [10] simulated the machining operations by using a finite element model. The machining forces are considered as area force and applied over the tool workpiece contact area. Liao [11] used the GA to find the optimal numbers of locators and clamps as well as their optimal positions in sheet metal assembly such that the workpiece deformation and variation are minimized. Amaral et al. [12] employed 3-2-1 locating method and developed an algorithm to automatically optimize fixture support, clamp locations, and clamping forces, to minimize workpiece deformation, subsequently increasing machining accuracy. Deiab and Elbestawi [13] presented the results of a full factorial experimental investigation of

* Corresponding author. Tel.: +381 21 485 23 26; fax: +381 21 454 495.
E-mail address: vukelic@uns.ac.rs (D. Vukelic).

0278-6125/$ – see front matter © 2013 The Society of Manufacturing Engineers. Published by Elsevier Ltd. All rights reserved.
http://dx.doi.org/10.1016/j.jmsy.2013.05.004

the tribological conditions of the workpiece–fixture elements contact surface for workholding applications taking into consideration the effect of workpiece material, workpiece surface roughness, fixture element roughness, and normal load. Deng and Melkote [14] presented a model-based framework for determining the minimum required clamping force to ensure the dynamic stability of a fixtured workpiece during machining. Kaya [15] presented a GA-based continuous fixture layout optimization method. The optimization objective was to search for a 2D fixture layout that minimizes the maximum elastic deformation at different locations of the workpiece. Siebenaler and Melkote [16] presented a fixture–workpiece model using FEA to investigate the influence of various parameters on workpiece deformation, including the compliance of the fixture body, contact friction, and mesh density. Tian et al. [17] presented an approach for optimally selecting the locating positions of workpieces and identifying feasible clamping regions that meet the requirements of the form-closure principle for fixture layout. Sanchez et al. [18] calculated the contact load distribution and valid clamping regions in machining processes. They also calculated the contact load using a non-iterative means by modelling both fixture and workpiece as separate and independent FEA problems. Ratchev et al. [19] addressed this knowledge gap by proposing a fixture–workpiece behaviour prediction methodology that utilized commercial FEA software for the prediction of complex fixture–workpiece behaviour during machining processes. Chen et al. [20] presented a fixture layout design and clamping force optimization procedure based on the GA and FEM. The optimization procedure was multi-objective: minimizing the maximum deformation of the machined surfaces and maximizing the uniformity of deformation. Padmanaban et al. [21] used an ant colony algotithm (ACA)-based discrete optimization method to optimize fixture layout under dynamic conditions. They also proved that in the fixture layout optimization ACA outperformed GA. Wang et al. [22] proposed a system based on FEA which compares the deformation induced by machining forces to the tolerance. System can mesh workpiece, assign material properties and boundary conditions, and create FEA files ready for calculation with limited human interference. Padmanaban et al. [23] optimized fixture layout for 2D workpiece geometry with an objective of minimizing the workpiece elastic deformation using ACA-based discrete and continuous fixture layout optimization methods. Hazarika et al. [24] developed a setup planning methodology for prismatic parts considering fixturing aspects. The objective function is formulated to minimize the maximum of locating elements reaction forces during machining and clamping. Layout optimization is formed as a constrained optimization problem and solved using nonlinear optimization technique. Vishnupriyan et al. [25] presented a method for determination of optimal fixture layout in order to minimize the machining error considering both locator geometric error and workpiece elastic deformation. Chaari et al. [26] presented a modelling methodology for geometrical machining defect. The kinematical deviation due to part locating and relocating is modelled by homogeneous transformation. Dynamic displacements caused by clamping and machining force are determined by FEA. Tadic et al. [27] proposed an approach to workpiece clamping based on intentional plastic deformation of workpiece in some predefined narrow zones. They analysed load capacity and compliance of these interfaces. Vishnupriyan [28] investigated the significance of system compliance and workpiece dynamics as the two critical sources of machining error. Considering different layouts and various clamping forces, the resulting components of machining error were computed. Selvakumar et al. [29] proposed a hybrid scheme to design an optimum fixture layout in order to reduce the maximum elastic deformation of the workpiece caused by the clamping and machining forces acting on the workpiece while machining.

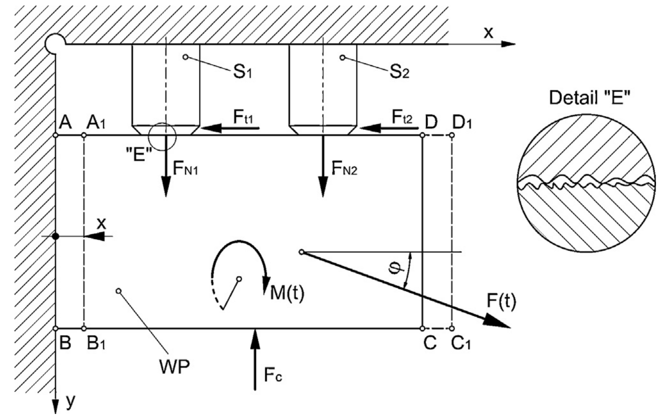

Fig. 1. Schematic drawing of fixture elements–workpiece interface compliance.

Several important conclusions stem from the analysis of previously discussed investigations. Namely, wrong or inadequate fixturing process can lead to elastic or plastic workpiece deformations, as well as to static and elastic displacements which can greatly influence final workpiece accuracy. On the other hand, inadequate clamping force can cause detachment of workpiece from locating elements during machining, leading to less efficient fixturing process. This is especially true when machining thin-walled and complex-geometry workpieces, where inaccuracy, deformations and distortions can be minimized through optimization of locating scheme (number, type, and displacement of locating elements) and clamping scheme (number, type, and displacement of clamping elements and clamping force dimensioning). Considering modern cutting regimes (high cutting speeds, exceeding 1000 m/min, high feed rates, sometimes over 1000 mm/min, large chip cross sections and cutting forces) special attention should be paid to fixture layout optimization which would allow minimization of workpiece–fixture interface compliance.

Current results in the domain of optimization of micro- and macro-geometry of clamping and locating fixture elements are not universally applicable. This is especially true considering the dynamic behaviour of contact interfaces between fixture elements and workpiece, i.e., tangential load capacity and interface load capacity. Investigations published so far, basically deal with dynamic behaviour analysis of fixture assembly. Thus, it is impossible to thoroughly analyze dynamic behaviour of a specific contact interface between clamping/locating elements and workpiece. The authors maintain that comprehensive analysis of dynamic behaviour and optimization of fixture elements requires, first of all, a dedicated measuring instrument which allows testing of physical models which represent clamping/locating elements and workpiece.With this in mind, investigations in the discussed area should be directed towards:

- development of a universal device to allow experimental investigation of fixture–workpiece interface compliance in dynamic conditions, i.e., with realistic simulation of contact interface loads, and
- investigation and analysis of dynamic fixture–workpiece interface compliance.

2. Methodology

It is often the case that the cutting forces in fixtures are counterbalanced by friction forces which occur on interface, surfaces between workpiece and clamping/locating elements. Shown in Fig. 1 is a workpiece (WP) which is located in the neighbourhood of some point on the direction *AB* by two locating elements (S_1 and

S_2). The workpiece is clamped to the locating surface by the clamping force, F_c. During machining, workpiece is exposed to dynamic cutting force, $F(t)$ and cutting moment, $M(t)$. Cutting force, $F(t)$, and cutting moment, $M(t)$, are functions of time and, in general, can attack any point on workpiece. Cutting force and moment can be of various magnitude, direction and sense. Thus, the locating elements are generally acted upon by normal reactions (F_{n1} and F_{n2}) and tangential forces (F_{t1} and F_{t2}), which are also known as the friction forces. When the cutting force, $F(t)$, and cutting moment, $M(t)$, are acting in the designated direction (Fig. 1), there shall occur certain displacement due to compliance of the contact interface between locating elements (S_1 and S_2) and workpiece, regardless of the magnitude of $F(t)$, and $M(t)$. This is well known from the relation which describes stress and deformation. The magnitude of displacement, x, is generally a function of a large number of parameters and can be stated as follows:

$$x = f[F(t), M(t), \varphi, F_{n1}, F_{n2}, M_{w1}, M_{w2}, M_{s1}, M_{s2}, G, K] \quad (1)$$

where: $F(t)$ – cutting force; $M(t)$ – cutting moment, F_{n1} and F_{n2} – normal reactions on locating elements; M_{w1} and M_{w2} – a set of parameters which define mechanical and thermal properties of workpiece material; M_{s1} and M_{s2} – a set of parameters which define mechanical and thermal properties of locating elements material; G – a set of parameters which define macro- and micro-geometry of locating element and workpiece interface surface; K – other interface-related conditions, such as machining with or without coolant and lubricant, machining errors, and other parameters.

Considering a large number of parameters which influence interface compliance and displacement x, given in expression (1), the interface compliance can be precisely determined only by experimental methods. It should be noted that interface compliance between fixture elements and workpiece is directly related to workpiece errors. Namely, if the displacement is $x \geq T$, where T represents the allowed machining tolerance of some functional measure relative to the locating surface, AB, (Fig. 1), this shall inevitably result in machining error.

Proposed in this paper is a radically different approach to the problem of interface compliance. Especially important for interface compliance is the dynamic behaviour of workpiece and fixture elements. According to that authors propose the development of a special device to allow investigation of displacements on physical models within particular contact interface zones under the influence of cutting forces of specified dynamic characteristics. In this way, it should be possible to combine various exchangeable clamping/locating elements and workpiece material specimens, use them as contact pairs to test their dynamic behaviour and perform optimization of interface load capacity, i.e., minimize interface compliance. The experimental data shall also be used to produce regression equations and consider the influence of macro- and micro-geometry of contact pairs, various fixture element materials, various magnitudes of cutting force, and other factors on contact interface compliance

Fig. 2 shows the schematic drawing of the device dedicated to testing of fixture–workpiece interface compliance. Exchangeable clamping/locating element, M, which was previously attached to its carrier, CM, is attached to workpiece material specimen, WP, which plays the role of the workpiece. In case of a spherical, pointed, and similar types of contacts, the contact interface is established in the neighbourhood of points K_1, K_2 and K_3. The element which locates the workpiece from three points, provides an even load distribution between particular elements. The contact interface can also be realized in the neighbourhood of particular lines, or over a surface – depending on the micro-geometry of contact pair. The interface contact is loaded by the carrier, CM, and the ball, B. Normal load (i.e. clamping force), F_n, is applied by the lever mechanism, L, which freely rotates about O_2–O_2 axis, and with calibrated weights,

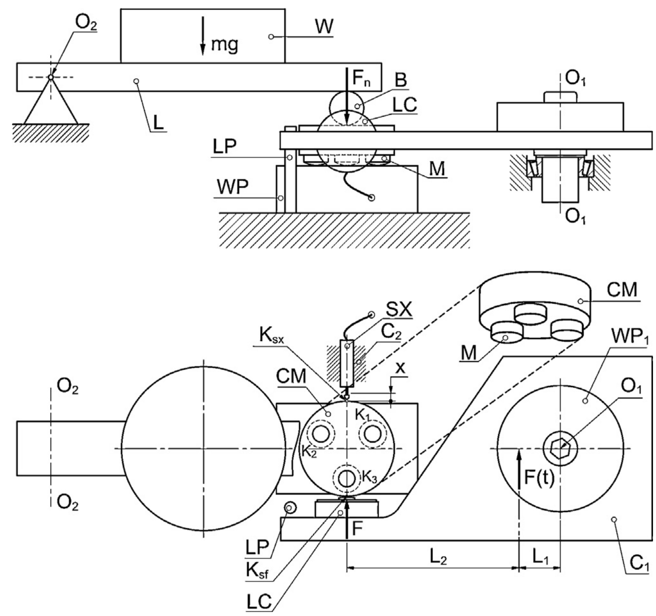

Fig. 2. Schematic drawing of the device for measurement of dynamic compliance of fixture–workpiece interface.

$W = mg$. Tangential load, F, i.e., component of cutting force, $F(t)$, is applied by the compression load cell, LC, mounted on the carrier, C_1, to which a workpiece material specimen, WP_1, is affixed. The carrier C_1 is pivoted about point O_1, i.e., axis O_1–O_1. Depending on the attack point of cutting force, $F(t)$, i.e., distances L_1 and L_2, a component of the cutting force $F(t)$ is transmitted by LC onto the carrier, CM, at point K_{sf}. Displacement of carrier CM, i.e., the exchangeable clamping/locating element, M, is registered by a displacement sensor, SX, which is mounted on the fixed carrier C_2. During displacement of exchangeable clamping/locating element, M, relative to workpiece material specimen, WP, the ball, B, is rolling along the carrier CM. Measurement error is the result of unregistered rolling friction force which occurs between the ball, B, and carrier, CM. According to calculations which are not presented here, and bearing in mind that rolling friction coefficient is much smaller than the sliding friction coefficient, there follows that the total measurement error does not exceed 1%. It should be noted that the device was designed so that this error is minimized. Shown in Fig. 3 is the auxiliary measurement instrumentation which consists of:

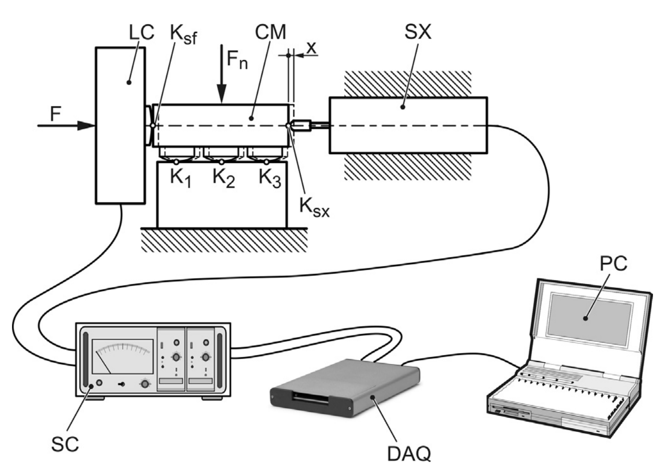

Fig. 3. System for the measurement of dynamic compliance of fixture–workpiece interface.

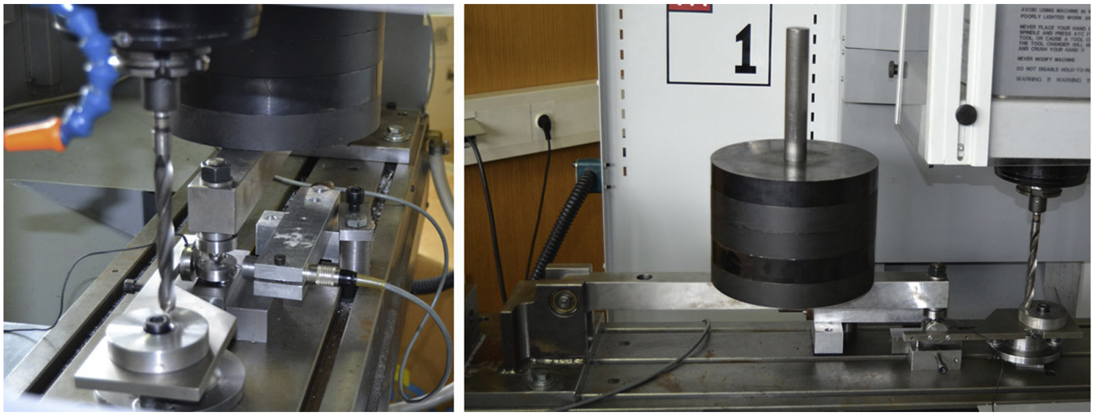

Fig. 4. Photo image of the device for model testing of dynamic behaviour of clamping/locating fixture elements.

- The compression load cell (shown as LC in Fig. 3) FC2311-0000-0250, with force range up to 1100 N, measuring tangential force, F, which is proportional to the cutting force, $F(t)$;
- The inductive displacement transducer W1T (shown as SX in Fig. 3), with accuracy of 0.017 μm, with nominal displacement of ±1 mm, and deviation of the sensitivity from normal sensitivity less than ±1%. Before the measurement, displacement transducer was calibrated on a tool microscope, UIM-21;
- The 2 channel HBM signal conditioner (shown as SC in Fig. 3) which processes the signals from sensors LC and SX;
- The 8 analogue input channels simultaneous sampling data acquisition module with a 16-bit resolution (shown as DAQ in Fig. 3), which was used for sampling of the signal from the LC and the SX; and, The PC which controls DAQ module and stores the results of measurement for further processing.

The developed device represents an important prerequisite for advanced research in the domain of compliance analysis and optimization of fixture elements for clamping and locating. The device offers several basic advantages:

- Contact load F is maintained at the exact, realistic level which matches that of the machining process. Cutting force can be generated in the process of milling, grinding or drilling on a workpiece material specimen, WP_1, which is made of a particular material of choice. In addition, cutting regime parameters and cutting tools can be selected according to requirements.
  Exchangeable clamping/locating element, M, can be of arbitrary geometry, micro geometry and material. The same applies to workpiece material specimen, WP.
- Contact pairs are of simple shape and are many times cheaper than a complete fixture assembly, especially bearing in mind the vast number of possible variations regarding parameters of influence.
- Machining can be performed with or without coolant and lubricant.

One essential advantage of this device is the possibility for a thorough dynamic analysis of the particular type of fixture–workpiece contact interface, with the influence of other fixture elements eliminated. This allows extensive comparison and optimization of particular interface types, opening the way to finding more reliable solutions of clamping/locating elements in terms of compliance reduction.

Shown in Fig. 4 are photo images of the device designed for model testing of dynamic behaviour of clamping/locating fixture elements.

3. Results

The specially designed device was subsequently used to conduct experimental investigation of the influence of spherical tip on the clamping/locating element on the compliance of fixture–workpiece interface. Exchangeable clamping/locating element (Fig. 5a) is made of EN 10083-1 steel, 56HRc, with a spherical tip in two variants: $R = 10$ mm and $R = 60$ mm. In both variants ($R = 10$ mm and $R = 60$ mm), the exchangeable elements were grinded so that their contact area has roughness of $R_a = 0.8$–1.0 μm. All elements were mounted onto the carrier shown in Fig. 5b.

Given in Fig. 6a and b. are photo images of a spherical-tip exchangeable clamping/locating element with its carrier, and the workpiece material specimen. Spherical-tip exchangeable elements (Fig. 6a) were used in the experiment to represent clamping/locating elements (three spherical-tip exchangeable elements are mounted into the carrier). Experimental investigations were performed using workpiece material specimens made of C 45 E (annealed), tensile strength 710 MPa and 208 HB hardness. Chemical composition of the steel was: 0.44%C; 0.18%Si; 0.27%Mn; 0.011%Si, and <0.010%P. Prismatic workpiece material specimen, 25 mm × 30 mm × 50 mm, was used in the experiment to represent workpiece (Fig. 6b).

Clamping forces, F_n, were varied within 278–631.2 N interval. For each particular value of clamping force, a twist drill, Ø12, was used at $n = 2000$RPM and varied feeds, f, to simulate various tangential forces. These forces and their corresponding feeds were monitored and recorded using the discussed measuring instrumentation.

Shown in Fig. 7a–c are recordings of all tangential forces, F, and corresponding displacements, x. The results of measurement are shown in Table 1.

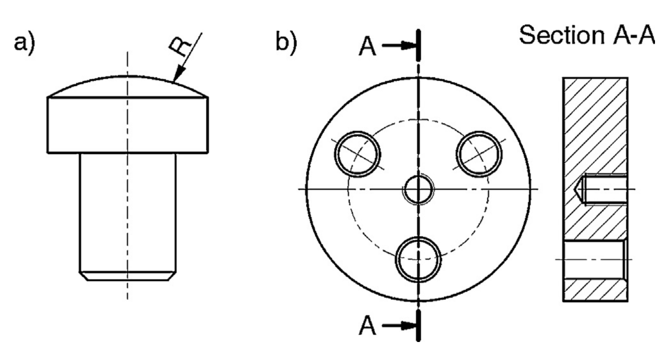

Fig. 5. 2D drawing: (a) exchangeable clamping/locating element, and (b) its carrier.

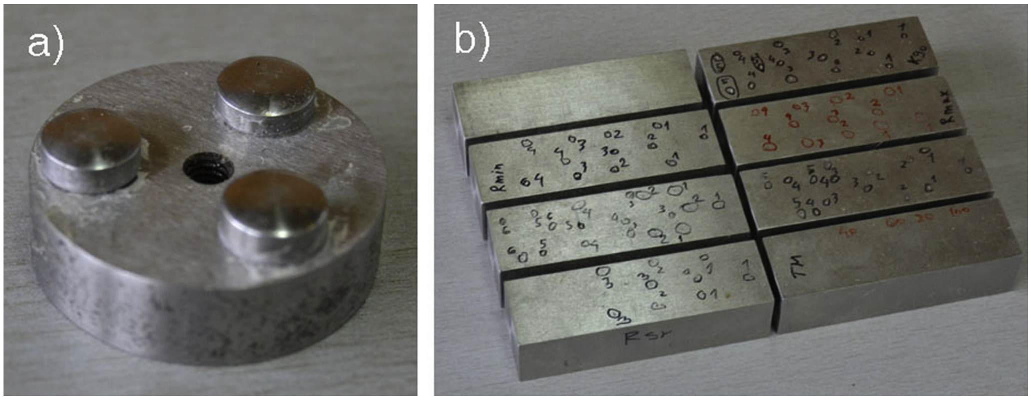

Fig. 6. Photo images: (a) exchangeable clamping/locating elements, and (b) workpiece material specimens.

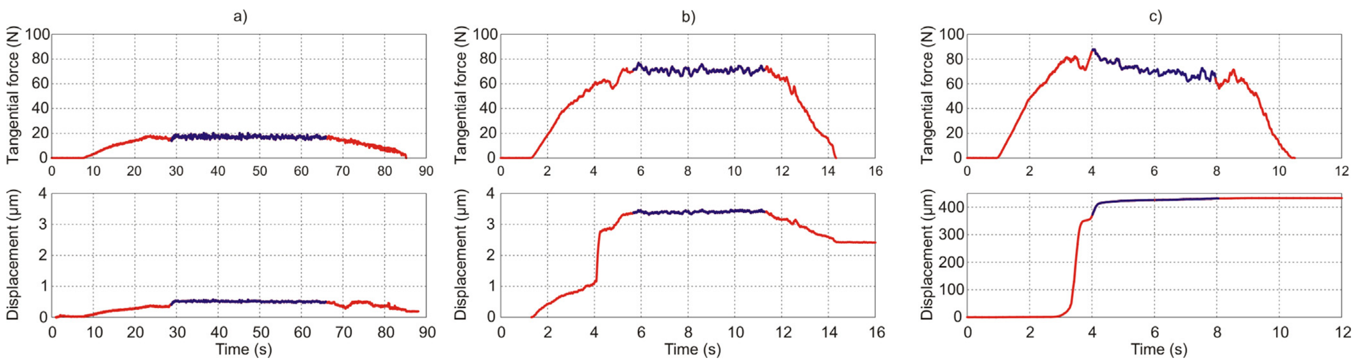

Fig. 7. Recordings of tangential forces, *F*, and corresponding displacements, *x*.

Table 1 contains the values of varied clamping forces, F_n, mean values of dynamic tangential force, $\bar{F}$, maximum dynamic tangential force, F_{max}, as well as the mean values of displacement, $\bar{x}$, and maximum displacement, x_{max}. The values from Table 1 pertain to the two radii of spherical tip (R = 10 mm and R = 60 mm). Based on the data from Table 1 it is evident that certain values of dynamic forces and displacement are missing. The missing values are the result of combinations of cutting and tangential forces which resulted in large displacements, exceeding 50 μm.

Also obvious from Table 1 is the fact that diagrams in Fig. 7a–c pertain to experiments numbered 1, 4, and 6, in case of clamping with R = 60 mm, at F_n = 631.2 N clamping force.

Fig. 8a and b presents 3D diagrams of dependence of mean tangential load, $\bar{F}$ (interface load capacity) on the normal load, F_n (clamping force) and mean value of displacement, $\bar{x}$, obtained for two different sphere radii (R = 10 mm and R = 60 mm). The diagrams in Fig. 8a and b were generated according to data in Table 1.

Correlation between mean tangential force, $\bar{F}$, clamping force, F_n, and mean displacement, $\bar{x}$, was established for both radii values of the spherical-tip clamping/locating element in the following form:

$$\bar{F} = (C_1 \cdot F_n + C_2 \cdot F_n^2 + C_3 \cdot F_n^3) \cdot \bar{x}^{C_4} \quad (2)$$

Based on regression equation (2) and the general expression for compliance, c ($c = x/F$, c – interface compliance, x – displacement, F

Table 1
Results of measurements of tangential forces, *F*, and corresponding displacements, *x*.

No.	F_n (N)	f (mm/min)	R = 10 (mm)				R = 60 (mm)			
			$\bar{F}$ (N)	F_{max} (N)	$\bar{x}$ (μm)	x_{max} (μm)	$\bar{F}$ (N)	F_{max} (N)	$\bar{x}$ (μm)	x_{max} (μm)
1	631.2	20	20.51	24.20	0.52	0.60	17.05	20.21	0.51	0.60
2	631.2	40	35.92	42.04	1.16	1.29	38.85	49.09	0.94	1.04
3	631.2	60	52.00	59.79	1.47	1.62	50.50	56.91	1.13	1.24
4	631.2	80	67.11	76.72	2.40	2.70	70.38	76.82	3.38	3.48
5	631.2	100	–	–	–	–	84.05	94.12	8.46	8.67
6	631.2	120	–	–	–	–	–	–	–	–
7	513.5	20	18.27	20.92	0.54	0.62	19.04	22.08	0.46	0.64
8	513.5	40	34.19	40.42	0.84	0.99	34.30	38.77	0.95	1.04
9	513.5	60	49.96	56.33	5.36	5.67	49.20	56.64	1.62	1.77
10	513.5	80	–	–	–	–	63.45	68.52	13.31	13.85
11	513.5	100	–	–	–	–	–	–	–	–
12	395.8	20	19.77	22.63	1.99	2.22	19.21	23.64	0.55	0.64
13	395.8	40	35.87	41.91	5.11	5.49	34.97	39.48	1.17	1.28
14	395.8	60	–	–	–	–	–	–	–	–
15	278.0	10	12.71	24.20	0.87	1.36	11.48	14.31	0.17	0.43
16	278.0	20	19.40	22.72	1.68	1.86	18.83	22.68	0.66	0.75
17	278.0	30	–	–	–	–	–	–	–	–

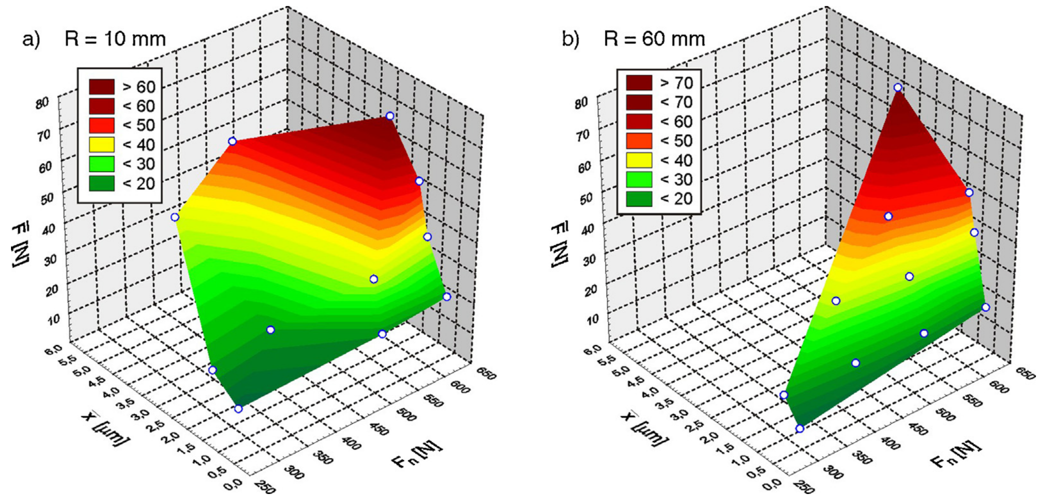

Fig. 8. 3D diagrams showing dependence of mean tangential load on the interface load capacity, $\bar{F}$, normal load F_n (clamping force) and mean interface compliance, $\bar{x}$, for two different radii of spherical-tip clamping elements, (a) R = 10 mm and (b) R = 60 mm.

– force causing displacement) one can establish the contact interface compliance, c, as the function of $\bar{x}$ and F_n, for both radii of the spherical-tip clamping/locating element:

$$c = \frac{\bar{x}}{\bar{F}} = \frac{\bar{x}}{(C_1 \cdot F_n + C_2 \cdot F_n^2 + C_3 \cdot F_n^3) \cdot \bar{x}^{C_4}} = \frac{\bar{x}^{1-C_4}}{(C_1 \cdot F_n + C_2 \cdot F_n^2 + C_3 \cdot F_n^3)} \quad (3)$$

Table 2 shows constant values, C_i (i = 1–4), spherical tip radii of the clamping/locating elements, (R), and the corresponding correlation coefficient, (r).

Using data from Table 1 and Fig. 9 shows a 2D rendering of the dependence of contact interface stiffness on the clamping force for both spherical tip radii of the clamping/locating elements. The rendering in Fig. 9 visually depicts the changes in contact interface stiffness as the function of clamping force, for both spherical-tip radii. For that reason, the diagram deals with contact interface stiffness, which, by definition, equals inverse value of contact interface compliance. Fig. 9 also shows clamping force, F_n, in (daN).

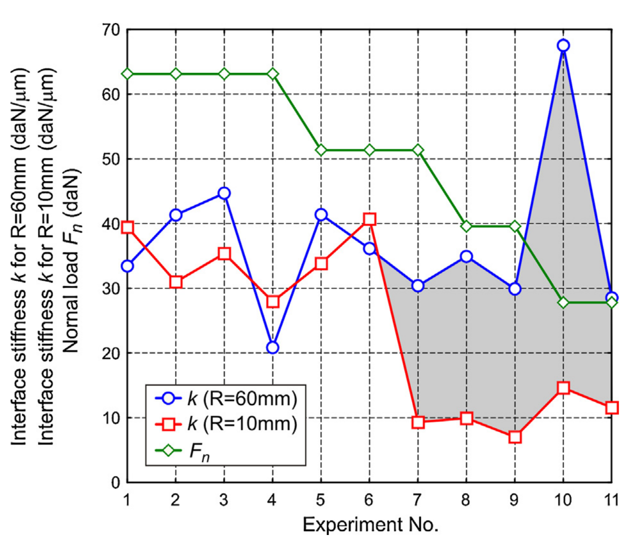

Fig. 9. Contact interface stiffness for two physical models of clamping elements with different spherical-tip radii.

4. Discussion

The specially designed device allows experimental testing of fixture–workpiece interface behaviour under dynamic loads, while eliminating the influence of all fixture elements other than the clamping/locating ones. For example, the influence of workpiece stiffness and fixture elements stiffness is thus successfully eliminated. This allowed following benefits:

- Reliable determination of interface compliance and load capacity of any type, for the selected dynamic load and clamping force;
- Experimental investigation of elements (physical models) with various macro- and micro-geometry of contact surfaces. For example, it is possible to investigate contact between two flat surfaces of various sizes, contact between spheres of various radii and a flat surface, contact pairs with various micro geometries, and other types of contacts. In this way, it is possible to conduct a thorough optimization of contact interfaces between clamping/locating elements and workpiece, thus producing highly reliable solutions.

Investigations of dynamic behaviour were conducted on a contact interface between sphere and flat surface. Exchangeable clamping/locating elements with spherical tips were used to represent the clamping/locating elements, while prismatic material specimens were used as workpieces. The goal of experimental investigation was to establish the influence of tip radius size on the contact interface compliance and load capacity. It should be noted that the experiments were performed with relatively lower values of clamping forces, F_n. This can be explained by the fact that this investigation was focused on locating and clamping of thin-walled workpieces. Fig. 7a–c illustrates the phenomenon of small displacements of specimens representing the clamping/locating elements CM, relative to workpiece WP, i.e., the occurrence of slipping and deformation of material in the contact areas under the influence of tangential forces of various magnitudes. Based on the typical signals of tangential forces and their corresponding displacements, it is possible to discern between three types of displacement:

- Type A displacement (Fig. 7a) when the system reverts to previous state upon force cancellation, while the displacements are small, on the micrometre order of magnitude;

Table 2
Constant values C_i (i = 1–4), spherical tip radii of the clamping/locating elements, (R), and the corresponding correlation coefficient, (r).

Element	Constant C_1	Constant C_2	Constant C_3	Constant C_4	Correlation coefficient r
R = 10 (mm)	1.25×10^{-1}	-3.938×10^{-4}	4.776×10^{-7}	0.501	0.939
R = 60 (mm)	1.746×10^{-1}	-4.458×10^{-4}	4.371×10^{-7}	0.3118	0.940

Table 3
Basic statistical parameters for the experimental data.

Element	$\bar{\bar{F}}$ (N)	SD($\bar{\bar{F}}$) (N)	$\bar{\bar{x}}$ (μm)	SD($\bar{\bar{x}}$) (μm)
R = 10 (mm)	33.24	17.25	1.99	1.71
R = 60 (mm)	33.07	18.19	1.04	0.87

- Type B displacement (Fig. 7b) when the system partially reverts to previous state upon force cancellation, regardless of the magnitude of displacement;
- Type C displacement (Fig. 7c) where total slipping occurs on the contact interface, in excess of 400 μm, which represents the limit set by the safety limit pin on the device (shown as LP in Fig. 2).

Obviously, in case of Type A displacement, the deformations of material in contact under tangential force, F, predominantly take place in the domain of elastic deformations. In the case of Type B displacement, there is a significant presence of plastic deformations of the material within the interface zone. Finally, Type C displacement means obvious disruption of contact due to sliding.

Regardless of displacement type, the recorded data were analysed using mean displacement and mean tangential force values (mean interface load capacity). This allowed objective comparison of different displacement types from the aspect of workpiece error.

The 3D diagrams in Fig. 8a and b it is evident that the contact established with a sphere, R = 60 mm, features higher load capacity and lower interface compliance compared with the contact established with R = 10 mm. This can be clearly seen in the diagrams (Fig. 8a and b) which were drawn to the same scale, i.e., within identical value ranges.

Basic statistical parameters for the experimental data are shown in Table 3. It includes: mean of $\bar{F}$ (Table 1), standard deviation of $\bar{F}$ (Table 1), mean of $\bar{x}$ (Table 1), and standard deviation of $\bar{x}$ (Table 1).

In this experimental investigation of interface compliance, there was no significant difference between the means ($\bar{\bar{F}} = 33.24$ N for sphere radius R = 10 mm, i.e., $\bar{\bar{F}} = 33.07$ N for sphere radius R = 60 mm) at the 95% confidence level. Dispersion of $\bar{\bar{F}}$ (R = 60 mm) (SD($\bar{\bar{F}}$) = 18.19 N) was larger than $\bar{\bar{F}}(R = 10\text{ nm})$ (SD($\bar{\bar{F}}$) = 17.25 N). This fact implies that the dynamic component of tangential force was much more intensive during experiments with R = 60 mm, than was the case with R = 10 mm. Regardless of that, $\bar{\bar{x}}$ of R = 60 mm was 48% lower, compared with $\bar{\bar{x}}$ of R = 10 mm. During experiments 5 and 10 (Table 1), while testing the spherical-tip locating element, R = 10 mm, a total slipping occurred, which was not the case with R = 60 mm.

The dependence of contact interface compliance on the clamping force for both spherical-tip radii, was established and expressed through regression Eq. (2) and the general expression for interface compliance (Eq. (3) and Table 2). Bearing in mind the relatively high correlation coefficient, this equation can be used to determine interface compliance depending on the clamping force, F_n, as well as to analyze the influence of the two different spherical tip radii of clamping/locating elements.

The diagram in Fig. 9 illustrates the very complex influence of clamping force and tip radius on contact interface stiffness. The diagram shows that in the domain of relatively large clamping forces (experiments1–6) the tested specimens representing physical models of clamping/locating elements do not exhibit significant differences from the aspect of contact interface stiffness. However, the specimens with tip radius R = 60 mm exhibit superior performance at smaller clamping force values (experiments 7–11).

Theoretical explanation of this phenomenon lies in the difference between contact pressures and various characteristics of contact surfaces which take place when locating and clamping a flat surface against the spherical surface of various radii. Given the normal load, the contact between a larger radius sphere and a flat surface occurs over a significantly larger surface area which results in lower specific contact pressure. It should be noted that, due to low values of clamping forces chosen to adjust to thin-walled workpiece, it was not possible to precisely determine the real values of contact surface areas. In other words, the indent marks on workpiece specimens (Fig. 6b) were small and it was quite likely that most of the contact deformations were elastic, and thus disappeared once the clamping force was zero. Obviously, such calculation would be highly approximate. However, it is clear from the theoretical standpoint that larger sphere radius provides larger contact surface area and lower specific contact pressure. With this in mind, it should be noted that numerous results [30,31] of tribological investigations imply that friction coefficient tends to increase with the reduction of contact pressure and increase of contact surface area. For this reason, the interface compliance follows the same trend, which is confirmed by the results of this investigation.

5. Conclusions

Based on the previous discussion it is possible to draw following conclusions:

- According to survey of literature, published analyses of interface compliance between clamping/locating elements and workpiece under dynamic loads have been mostly confined within the analysis of dynamic behaviour of fixture assemblies. However, such investigations are devoid of universal character and do not allow optimization of material and macro-/micro-geometry of the clamping/locating elements with interface compliance or tangential load capacity as the goal function.
- The device which was specially designed in this investigation for the purpose of testing the dynamic behaviour of clamping/locating fixture elements, allows testing of physical models which represent clamping/locating elements and workpiece, and offers wide possibilities for investigations in this area.
- The results of experimental investigations presented in this paper have shown that the proposed measuring device allows a significant leap forward in the domain of optimization of the types of contact interfaces between clamping/locating fixture elements and workpiece. This allows increase of tangential loads, and decrease of interface compliance.
- The results can find a very significant application in industry, allowing redesign of clamping/locating fixture elements in order to increase fixture–workpiece load capacity and lower interface compliance. Positive effects of such redesign lie in the higher reliability of fixtures, increased machining accuracy or higher productivity based on more intensive cutting regimes.
- The authors maintain that future investigations should be directed towards optimization of contact macro- and micro-geometry, as well as towards selection of materials for

clamping/locating fixture elements. Moreover, it would be of special importance to focus on experimental investigations of the behaviour of interface compliance under intensive cooling and lubrication of workpiece during machining. More precisely, it is highly likely that lubrication of contact surfaces on workpiece and standard clamping/locating fixture elements (with flat or spherical contact surface) boosts the interface compliance. Under such circumstances, it would be very useful to apply clamping/locating fixture elements which slightly penetrate the workpiece surface, causing only minor aesthetic changes, while allowing significant increase in fixture–workpiece load capacity.

References

[1] Bi ZM, Zhang WJ. Flexible fixture design and automation: review, issues and future directions. International Journal of Production Research 2001;39:2867–94.

[2] Wardak KR, Tasch U, Charalambides PG. Optimal fixture design for drilling through deformable plate workpieces. Part I. Model formulation. Journal of Manufacturing Systems 2001;20:23–32.

[3] Meyer RT, Liou FW. Fixture analysis under dynamic machining. International Journal of Production Research 1997;35:1471–89.

[4] Nee AYC, Kumar AS, Tao ZJ. Intelligent fixture with a dynamic clamping scheme. Proceedings of the Institution of Mechanical Engineers, Part B: Journal of Engineering Manufacture 2000;214:183–96.

[5] Li B, Melkote SN. Fixture clamping force optimization and its impact on workpiece location accuracy. International Journal of Advanced Manufacturing Technology 2001;17:104–13.

[6] Hurtado JF, Melkote SN. A model for synthesis of the fixturing configuration in pin-array type flexible machining fixtures. International Journal of Machine Tools and Manufacture 2002;42:837–49.

[7] Kulankara K, Satyanarayana S, Melkote SN. Iterative fixture layout and clamping force optimization using the genetic algorithm. Journal of Manufacturing Science and Engineering: ASME 2002;124:119–25.

[8] Vallapuzha S, DeMeter EC, Choudhuri S, Khetan RP. An investigation into the use of spatial coordinates for the genetic algorithm based solution of the fixture layout optimization problem. International Journal of Machine Tools and Manufacture 2002;42:265–75.

[9] Xiong CH, Xiong YL, Wang MY. Clamping planning in workpiece–fixture systems. In: Proceedings of ASME International Mechanical Engineering Congress and Exhibition (IMECE2003). 2003. p. 267–72.

[10] Kaya N, Ozturk F. The application of chip removal and frictional contact analysis for workpiece–fixture layout verification. International Journal of Advanced Manufacturing Technology 2003;21:411–9.

[11] Liao YG. A generic algorithm-based fixture locating positions and clamping schemes optimization. Proceedings of the Institution of Mechanical Engineers – Part B: Journal of Engineering Manufacture 2003;217:1075–83.

[12] Amaral N, Rencis JJ, Rong Y. Development of a finite element analysis tool for fixture design integrity verification and optimisation. International Journal of Advanced Manufacturing Technology 2005;25:409–19.

[13] Deiab IM, Elbestawi MA. Experimental determination of the friction coefficient on the workpiece–fixture contact surface in workholding applications. International Journal of Machine Tools and Manufacture 2005;45:705–12.

[14] Deng HY, Melkote SN. Determination of minimum clamping forces for dynamically stable fixturing. International Journal of Machine Tools and Manufacture 2006;46:847–57.

[15] Kaya N. Machining fixture locating and clamping position optimization using genetic algorithms. Computers in Industry 2006;57:112–20.

[16] Siebenaler SP, Melkote SN. Prediction of workpiece deformation in a fixture system using the finite element method. International Journal of Machine Tools and Manufacture 2006;46:51–8.

[17] Tian S, Huang Z, Chen L, Wang Q. A feature-based approach for optimal workpiece localization and determination of feasible clamping regions. International Journal of Advanced Manufacturing Technology 2006;30: 76–86.

[18] Sanchez H, Estrems M, Faura F. Fixturing analysis methods for calculating the contact load distribution and the valid clamping regions in machining processes. International Journal of Advanced Manufacturing Technology 2006;29:426–35.

[19] Ratchev S, Phuah K, Liu S. FEA-based methodology for the prediction of part-fixture behaviour and its applications. Journal of Materials Processing Technology 2007;191:260–4.

[20] Chen W, Ni L, Xue J. Deformation control through fixture layout design and clamping force optimization. International Journal of Advanced Manufacturing Technology 2008;38:860–7.

[21] Padmanaban KP, Prabhaharan G. Dynamic analysis on optimal placement of fixturing elements using evolutionary techniques. International Journal of Production Research 2008;46:4177–214.

[22] Wang Y, Xie J, Wang Z, Gindy N. A parametric FEA system for fixturing of thin-walled cylindrical components. Journal of Materials Processing Technology 2008;205:338–46.

[23] Padmanaban KP, Arulshri KP, Prabhakaran G. Machining fixture layout design using ant colony algorithm based continuous optimization method. International Journal of Advanced Manufacturing Technology 2009;45: 922–34.

[24] Hazarika M, Dixit US, Deb S. A setup planning methodology for prismatic parts considering fixturing aspects. International Journal of Advanced Manufacturing Technology 2010;51:1099–109.

[25] Vishnupriyan S, Majumder MC, Ramachandran KP. Optimal fixture parameters considering locating errors. International Journal of Production Research 2011;49:6343–61.

[26] Chaari R, Abdennadher M, Louati J, Haddar M. Modelling of the 3D machining geometric defects accounting for workpiece vibratory behaviour. International Journal of Simulation Modelling 2011;10:66–77.

[27] Tadic B, Jeremic B, Todorovic P, Vukelic D, Proso U, Mandic V, et al. Efficient workpiece clamping by indenting coneshaped elements. International Journal of Precision Engineering and Manufacturing 2012;13: 1725–35.

[28] Vishnupriyan S. Effect of system compliance and workpiece dynamics on machining error. Assembly Automation 2012;32:175–84.

[29] Selvakumar S, Arulshri KP, Padmanaban KP, Sasikumar KSK. Design and optimization of machining fixture layout using ANN and DOE. International Journal of Advanced Manufacturing Technology 2012:4281–2, doi: 10. 1007/s00170-012-.

[30] Aleksandrovic S, Nedeljkovic B, Stefanovic M, Milosavljevic D, Lazic V. Tribological properties of steel and al-alloys sheet metals intended for deep drawing. Tribology in Industry 2009;31:11–6.

[31] Marjanovic N, Ivkovic B, Stojanovic B, Blagojevic M. Disk on disk test of gear pair power losses. Tribology in Industry 2010;32:10–6.